

THE EFFECT OF STELLAR MIGRATION ON GALACTIC CHEMICAL EVOLUTION: A HEURISTIC APPROACH

EMANUELE SPITONI¹, DONATELLA ROMANO², FRANCESCA MATTEUCCI^{1,3,4}, AND LUCA CIOTTI⁵

Submitted August 25, 2018

ABSTRACT

In the last years, stellar migration in galactic discs has been the subject of several investigations. However, its impact on the chemical evolution of the Milky Way still needs to be fully quantified. In this paper, we aim at imposing some constraints on the significance of this phenomenon by considering its influence on the chemical evolution of the Milky Way thin disc. We do not investigate the physical mechanisms underlying the migration of stars. Rather, we introduce a simple, heuristic treatment of stellar migration in a detailed chemical evolution model for the thin disc of the Milky Way, which already includes radial gas flows and reproduces several observational constraints for the solar vicinity and the whole Galactic disc. When stellar migration is implemented according to the results of chemodynamical simulations by Minchev et. al. (2013) and finite stellar velocities of 1 km s^{-1} are taken into account, the high-metallicity tail of the metallicity distribution function of long-lived thin-disc stars is well reproduced. By exploring the velocity space, we find that the migrating stars must travel with velocities in the range $0.5 - 2 \text{ km s}^{-1}$ to properly reproduce the high-metallicity tail of the metallicity distribution. We confirm previous findings by other authors that the observed spread in the age-metallicity relation of solar neighbourhood stars can be explained by the presence of stars which originated at different Galactocentric distances, and we conclude that the chemical properties of stars currently observed in the solar vicinity do suggest that stellar migration is present to some extent.

Subject headings: Galaxy: abundances – Galaxy: evolution – Galaxy: disc – Galaxy: kinematics and dynamics

1. INTRODUCTION

Chemical evolution models are fundamental tools to understand the formation and evolution of the Milky Way (e.g. Matteucci 2001). A good agreement between model predictions and observed properties of the Galaxy is usually obtained by assuming that the disc is well described by concentric annular regions forming by continuous infall of gas without any exchange of matter between them (e.g. Matteucci & François 1989; Chiappini et al. 1997; François et al. 2004, among many others).

However, in the presence of gas infall, the Galactic disc cannot be adequately described by a model with non-interacting zones (see, e.g., Spitoni & Matteucci 2011, and references therein). In particular, radial motions of gas should be taken into account when the infalling gas has a specific angular momentum lower than that of the matter moving on circular orbits in the disc, so that mixing with the gas in the disc induces a net radial inflow. Lacey & Fall (1985) estimated that the gas inflow velocity is approximately 1 km s^{-1} at 10 kpc. Other internal mechanisms, in principle able to induce radial gas flows, may also be present in disc galaxies, as a consequence of asymmetric drift (Smet, Posacki & Ciotti 2014). Goetz

& Koeppen (1992), Portinari & Chiosi (2000), Spitoni & Matteucci (2011), Bilitewski & Schönrich (2012), Spitoni et al. (2013), Mott et al. (2013) and Cavichia et al. (2014) present chemical evolution models with the inclusion of radial gas flows. All these works generally agree on the magnitude and patterns needed for the gas velocities to fit the observational data: the maximum velocity must not exceed a few km s^{-1} .

On the other hand, in all the models cited above the stars are assumed to remain at their birth radii. The effect of the interaction of the stars with the spiral arms on the stellar orbits is discussed by Sellwood & Binney (2002), who show that: a) stars on circular orbits experience larger angular momentum changes, and consequently suffer more radial migration, than stars on low-angular momentum orbits; b) stars can migrate to large distances within discs, whilst remaining on nearly circular orbits. By studying the specific case of the Milky Way, Sellwood & Binney (2002) found that old stars formed in the solar neighbourhood may have been scattered nearly uniformly within the annular region between 4 and 12 kpc from the Galactic centre – a scenario confirmed qualitatively by subsequent studies. For instance, Röskar et al. (2008, 2012), using high-resolution N-body simulations coupled with smoothed particle hydrodynamics (SPH), have shown that stars can migrate across large Galactocentric distances due to resonant scattering with spiral arms, while remaining on almost circular orbits. The spiral perturbations redistribute angular momentum within the disc and lead to substantial radial displacements of individual stars, in a manner that largely preserves the circularity of their orbits. These models are able to explain the observed flatness and spread in

Emanuele Spitoni spitoni@oats.inaf.it

¹ Dipartimento di Fisica, Sezione di Astronomia, Università di Trieste, via G.B. Tiepolo 11, I-34131, Trieste, Italy

² I.N.A.F., Osservatorio Astronomico di Bologna, Via Ranzani 1, I-40127 Bologna, Italy

³ I.N.A.F. Osservatorio Astronomico di Trieste, via G.B. Tiepolo 11, I-34131, Trieste, Italy

⁴ I.N.F.N. Sezione di Trieste, via Valerio 2, 34134 Trieste, Italy

⁵ Dipartimento di Fisica e Astronomia, Università di Bologna, viale Berti-Pichat 6/2, 40127 Bologna, Italy

the age-metallicity relation of solar neighbourhood stars. Recent work by Vera-Ciro et al. (2014) confirm that stellar migration can be driven by Sellwood & Binney’s (2002) corotation scattering process.

All the above mentioned dynamical models do not consider the effect of the Galactic bar; the role of the bar for radial migration is thoroughly analysed in Minchev & Famaey (2010) and Minchev et al. (2011). These authors suggest that radial migration results from the nonlinear coupling between the bar and the spiral waves and predict a variation of the efficiency of migration with time and Galactocentric radius. In a more recent study, Halle et al. (2015) confirm that strong radial migration has to be expected in the case of a bar-spiral resonance overlap, but also suggest that the Galactic outer Lindblad resonance acts as a barrier: stars do not migrate from the inner to the outer disc, and vice versa⁶.

Although the existence of the phenomenon of radial migration seems to be established beyond any doubt, *a quantitative estimate of its impact on the chemical evolution of the Galactic disc is much more difficult*. Besides the above-mentioned work of Halle et al. (2015), that challenges any scenario in which significant fractions of stars move from the inner to the outer disc, and vice versa, some concerns about the effective role of the bar in stellar migration have been raised by Sánchez-Blázquez et al. (2014). These authors present a comparative study of the stellar metallicity gradients and age distributions in a sample of nearly face-on spiral galaxies, with and without bars. The process of radial migration should flatten the stellar metallicity gradient with time and, therefore, flatter stellar metallicity gradients should be expected in barred galaxies. However, Sánchez-Blázquez and collaborators do not find any difference in the metallicity nor in the age gradients of galaxies with or without bars.

The first attempt to analyse the impact that stellar migration could have on the chemical properties of the Milky Way disc was done by François & Matteucci (1993). By discussing the spread observed in the age-metallicity relation and in the $[\alpha/\text{Fe}]$ versus $[\text{Fe}/\text{H}]$ relations for solar neighbourhood stars, these authors concluded that most of the observed spread can be accounted for by the fact that some of the stars we observe at the present time in the solar vicinity might have been born in different regions of the Galactic disc, in particular in more inner ones. Their paper was based on observational features of a possible radial migration presented in pioneering works by Grenon (1972, 1989). Grenon identified an old population of super metal-rich stars, that are currently located in the solar vicinity, but have kinematics and abundance properties indicative of an origin in the inner Galactic disc.

Despite the recent advances in the field of galaxy formation and evolution, there are currently no self-consistent simulations containing the level of chemical implementation required for making detailed predictions for the number of ongoing and planned Milky Way observational campaigns. Even in high-resolution N-body experiments, one particle represents $\approx 10^{4-5}$ solar masses. Hence, a number of approximations are necessary to com-

pute the chemical enrichment self-consistently inside a dynamical simulation.

Schönrich & Binney (2009a,b) included in a chemical model the radial migration of stars and gas through the disc of the Galaxy by means of a probabilistic approach constrained by Milky Way observables and found results in agreement with Röskar et al. (2008). They found also that most observational properties and peculiarities of the thick disc could be explained by radial migration. Recently, Minchev et al. (2013, 2014) have presented a new approach for combining chemistry and dynamics that overcomes the technical problems originated by fully self-consistent simulations, and avoids the star formation and chemical enrichment problems encountered in previous simulations. They assume that each particle is one star and implement the star formation history and chemical enrichment deriving from a classic chemical evolution model for the thin disc into the simulated Galactic disc. Kubryk et al. (2013, 2014) also studied radial migration and chemical evolution for a general bar-dominated disc galaxy, by analysing the results of a fully self-consistent, high-resolution N-body+SPH simulation. Stars undergo substantial radial migration at all times, caused first by transient spiral arms and later by the bar. The authors stress that, despite the important amount of radial migration occurring in their model, its impact on the chemical properties is limited.

Here, we adopt a phenomenological approach to study the effects of different prescriptions for the stellar migration on the best known chemical evolution observables. In practice, we implement stellar migration in a very simple way in a detailed chemical evolution model for the Galactic thin disc that already includes radial gas flows. We first focus on the metallicity distribution function of long-lived stars in the solar neighbourhood. We then examine the effects of the migration on other observables, such as the age-metallicity relation of stars in the solar vicinity and the stellar density profile across the disc.

The paper is organised as follows: in Section 2 we describe our reference chemical evolution model and the way in which the radial gas flows and the stellar migration have been implemented. In Section 3 we report the model results without stellar migration, whereas model results with stellar migration are presented in Section 4. Finally, we draw our main conclusions in Section 5.

2. THE CHEMICAL EVOLUTION MODEL

Our reference model for the Galactic thin disc is that presented in Spitoni & Matteucci (2011). The model assumes that the disc grows via smooth accretion of gas of primordial chemical composition. The infall law is:

$$A(r, t) = a(r)e^{-\frac{t}{\tau_D}}, \quad (1)$$

where τ_D , the e -folding timescale, is a free parameter of the model and the coefficient $a(r)$ is set by the requirement that the current total mass surface density profile of the Galactic thin disc is reproduced. In order to mimic an inside-out formation of the disc (Larson 1976), the timescale for mass accretion is assumed to increase with the Galactic radius following a linear relation (see Chiappini et al. 2001, and references therein):

$$\tau_D(r) = 1.033r(\text{kpc}) - 1.27 \text{ Gyr}; \quad (2)$$

⁶ According to Dehnen (2000), the outer Lindblad resonance lies in the vicinity of the Sun.

TABLE 1
CHEMICAL EVOLUTION MODELS

Models	τ_D [Gyr]	ν [Gyr ⁻¹]	Radial gas inflow [km s ⁻¹]	Stellar migration	Stellar velocities [km s ⁻¹]
REF1	1.033 R[kpc]-1.27	variable (see Figure 1)	1	/	/
REF2	1.033 R[kpc]-1.27	1	1	/	/
'Minchev case'	1.033 R[kpc]-1.27	variable (see Figure 1)	1	10 % from 4 kpc 20 % from 6 kpc 60 % from 8 kpc	0.5, 1, 2

this relation holds for Galactocentric distances between 4 and 16 kpc. The region within 4 kpc is not considered in this paper. The infall law adopted in this work is clearly a rough approximation of the true mass assembly history of the disc, still necessary since we do not rely on a full cosmological setting. However, it has been shown (Colavitti et al. 2008) that the results of a model assuming such an exponentially-decaying infall law are fully compatible with those obtained with cosmological accretion laws.

As for the IMF, we use that of Scalo (1986), constant in time and space. We indicate with τ_m the evolutionary lifetime of the stars with initial mass m (Maeder & Meynet 1989). The Type Ia supernova (SN) rate is computed following Greggio & Renzini (1983) and Matteucci & Greggio (1986). The stellar yields are taken from Woosley & Weaver (1995) for core-collapse SNe, van den Hoek & Groenewegen (1997) for low- and intermediate-mass stars, and Iwamoto et al. (1999) for Type Ia SNe. We use a star formation (SF) rate proportional to the gas surface density:

$$\psi(r, t) \propto \nu \sigma_{gas}^k(r, t) \quad (3)$$

where ν is the efficiency of the SF process and $\sigma_{gas}(r, t)$ is the gas surface density at a given position and time. The exponent k is fixed to 1.4 (see Kennicutt 1998).

Motivated by the theory of SF induced by spiral density waves in galactic discs (Wyse & Silk 1989), we consider a variable star formation efficiency (SFE) as a function of the Galactocentric distance, $\nu \propto 1/r$ (model REF1, Table 1). This is different from Spitoni & Matteucci (2011), who use a constant value for the SFE (model REF2, Table 1). The reason for this choice is related to the fact that with a constant SFE the predicted abundance ratio patterns (e.g. [O/Fe] vs [Fe/H]) do not change much from radius to radius, thus making the hypothesis of stellar migration as a solution for the observed spread rather unlikely. Figure 1 shows the SFE as a function of the Galactocentric distance used in this work. It is worth emphasising that a larger SFE in the inner disc is assumed also by Kubryk et al. (2014) and, probably, by Minchev et al. (2013); in the latter paper the authors do not state it explicitly, but an inspection of their results leads us to believe that this is the case. It is the combination of radial migration with a variable SFE across the disc that allows to reproduce the observed abundance spreads.

2.1. The implementation of the gas radial flows

In our reference model a constant radial inflow of gas with velocity of -1 km s⁻¹ is implemented following the

prescriptions of Spitoni & Matteucci (2011).

We define the k -th shell in terms of the Galactocentric radius r_k , its inner and outer edge being labeled as $r_{k-\frac{1}{2}}$ and $r_{k+\frac{1}{2}}$. We take the inner edge of the k -shell, $r_{k-\frac{1}{2}}$, at the midpoint between the characteristic radii of the shells k and $k-1$, and similarly for the outer edge $r_{k+\frac{1}{2}}$. The flow velocities $v_{k+\frac{1}{2}}$ are assumed to be positive outward and negative inward.

Radial inflows with a flux $F(r)$ contribute to alter the gas surface density σ_{gk} in the k -th shell according to

$$\left[\frac{d\sigma_{gk}}{dt} \right]_{rf} = - \frac{F(r_{k+\frac{1}{2}}) - F(r_{k-\frac{1}{2}})}{\pi \left(r_{k+\frac{1}{2}}^2 - r_{k-\frac{1}{2}}^2 \right)}, \quad (4)$$

where the gas flow at $r_{k+\frac{1}{2}}$ can be written as

$$F(r_{k+\frac{1}{2}}) = -2\pi r_{k+\frac{1}{2}} v_{k+\frac{1}{2}} \sigma_{g(k+1)}. \quad (5)$$

We assume that there are no flows from the outer parts of the disc where there is no SF. In our implementation of the radial inflow of gas, only the gas in the Galactic disc at $r < 20$ kpc can move inward by radial inflow.

2.2. Including stellar migration in our chemical evolution model

As discussed in the Introduction, we implement stellar migration in our chemical evolution code using a phenomenological approach, without a specific description of the complex dynamical mechanisms affecting stellar orbits in galactic discs. In practice, we simply move stars formed at a given radius, with a certain age and a certain metal content, to the solar vicinity, according to some simple rule. Following the work of Kordopatis et al. (2013), we assume as a representative value for the velocity of the stars 1 km s⁻¹, that is $\simeq 1$ kpc Gyr⁻¹. To explore the velocity parameter space we also run models with stellar velocities fixed to 0.5 and 2 km s⁻¹.

We stress that by taking into account a velocity of 1 km s⁻¹, only stars with stellar lifetimes $\tau_m \geq 1$ Gyr, corresponding to initial masses $m \leq 2 M_\odot$ (see figure 3 of Romano et al. 2005, and references therein), can travel for distances larger than 1 kpc. We can thus safely assume that most of the metals produced by a stellar generation are ejected well within 1 kpc from their progenitors' birthplace. Therefore, the metal enrichment of the ISM in the solar vicinity is practically unaffected by the stars born in the inner regions, that are thus only 'passive tracers' of the process of migration. We notice that, as estimated by Lacey & Fall (1985) with simple calculations, the magnitude of the radial gas flows velocity is roughly

1 km s⁻¹ at 10 kpc. Hence, stellar migration and radial gas inflows are characterised by the same time scales, and this is the reason why one has to consider both processes for a complete and consistent study.

First, we want to test the effect of assuming a physically plausible stellar migration on our chemical evolution model predictions. To this aim, we use the results of chemo-dynamical simulations by Minchev et al. (2013) to obtain general recipes to be used in our pure chemical evolution code. We choose this study since the chemical evolution model adopted by the authors is very similar to ours, which allows a test of the validity of our approach. Indeed, as we will show in Section 4, if we assume that 10% and 20% of the stars born at 4 and 6 kpc, respectively, migrate towards 8 kpc, while 60% of those born at 8 kpc leave the solar neighbourhood (percentages are drawn from Minchev et al.’s dynamical simulations), the metallicity distribution function we predict for long-lived solar vicinity stars turns out to be very similar to that obtained by Minchev and collaborators.

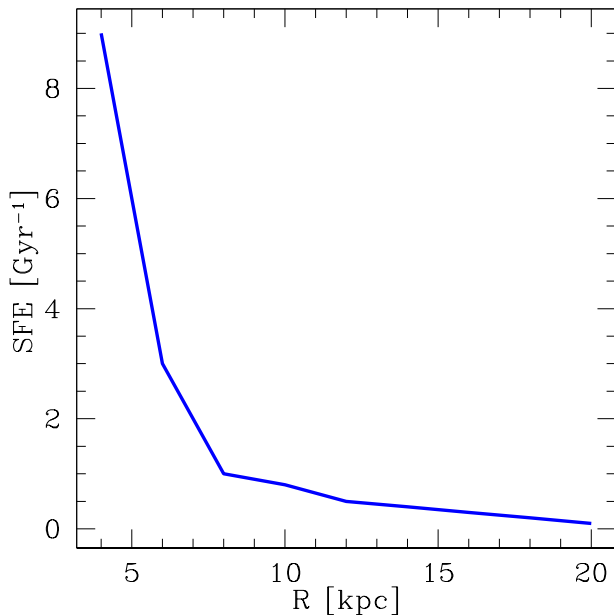


FIG. 1.— Adopted star formation efficiency as a function of Galactocentric radius for our models (except model REF2, that assumes a constant star formation efficiency).

Then, we also test some extreme cases, that are not supported by dynamical studies, with the aim of exploring the effects that a huge migration of stars would have on the chemical evolution of the solar neighbourhood (see Section 4).

3. MODEL RESULTS WITHOUT STELLAR MIGRATION

In this section, we present the results of our chemical evolution model including radial gas flows, either with variable (model REF1) or constant SFE (model REF2).

In Table 1, the principal characteristics of the models are reported: the time scale of thin-disc formation, τ_D , is listed in column 2; the adopted SFEs in column 3; the velocity of the radial gas inflow in column 4. For the model including stellar migration (‘Minchev case’ model), columns 5 and 6 specify the adopted prescrip-

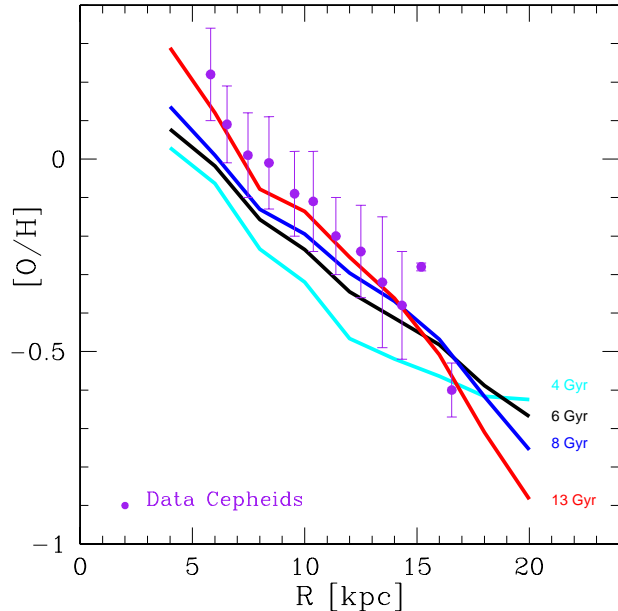


FIG. 2.— Evolution in time of the oxygen abundance gradient along the Galactic disc for our reference model in the presence of radial gas flows and variable star formation efficiency (model REF1); shown are the predictions of the model at 4, 6, 8 and 13 Gyr. The model results are compared to data from Cepheids (Luck & Lambert 2011), that track the present-day gradient.

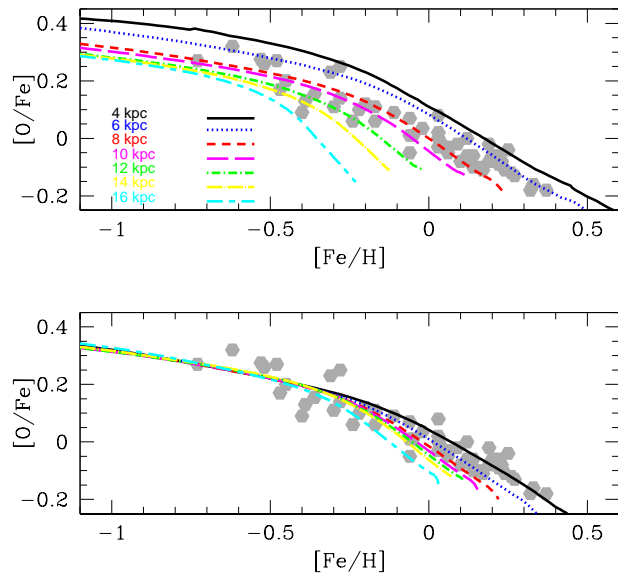


FIG. 3.— [O/Fe] vs [Fe/H] relations (lines) predicted by our models REF1 (*upper panel*) and REF2 (*lower panel*) at different Galactocentric distances, as indicated in the bottom left legend in the top panel. The two models include radial gas flows and differ only in the assumed SFE (see text). The data (symbols in both panels) refer to solar neighbourhood thin-disc stars and are taken from Bensby et al. (2005).

tions about the fraction of migrating stars and their velocities.

In Figure 2 it is shown that model REF1 (red curve, labelled 13 Gyr) perfectly fits the present-day oxygen abundance gradient measured in Cepheids. The data

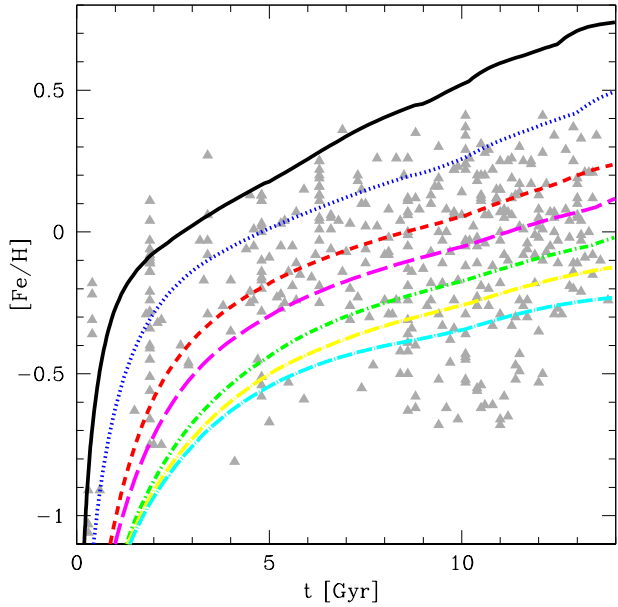


FIG. 4.— Temporal evolution of $[\text{Fe}/\text{H}]$ for our best model REF1 with radial gas flows and variable SFE, at different Galactocentric distances (curves; see Figure 3, upper panel, for the legend). Also shown are data by Bensby et al. (2014) for solar neighbourhood stars (symbols).

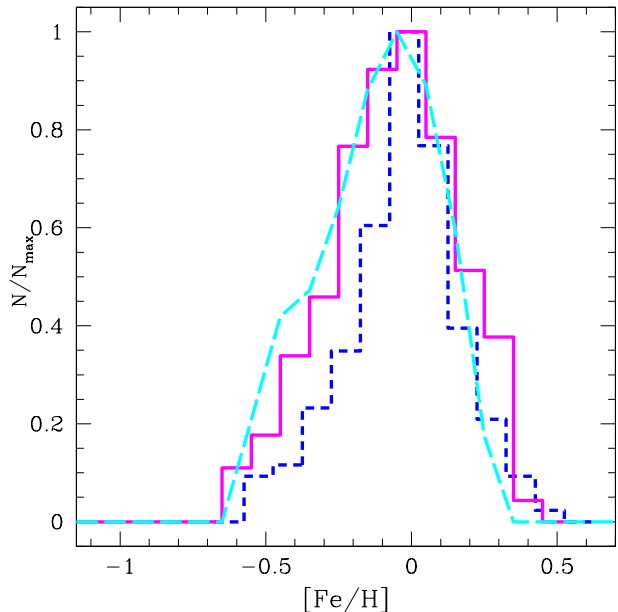


FIG. 5.— The G-dwarf metallicity distribution predicted by model REF1 (dashed line), that does not include stellar migration but includes a constant radial gas inflow of 1 km s^{-1} , is compared to the observed distributions of thin-disc stars by Adibekyan et al. (2013; solid magenta histogram) and Fuhrmann (2011; short-dashed blue histogram).

(from Luck & Lambert 2011) have been divided into bins 1-kpc wide; for each bin we compute the average value and the relative standard deviation. In Figure 2 we also show the evolution of the gradient, computed at 4, 6, 8 and 13 Gyr. It is worth noting that the combination of a variable SFE –with higher values in the inner disc

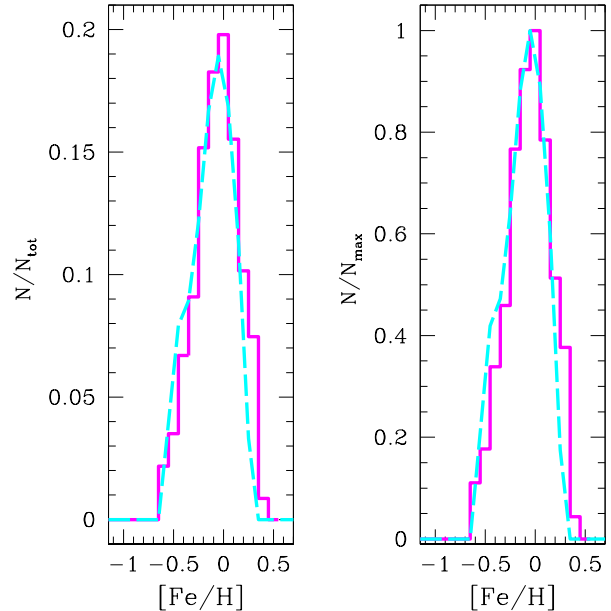


FIG. 6.— The G-dwarf metallicity distribution predicted by model REF1 without stellar migration (dashed line) is compared to the observed one by Adibekyan et al. (2013; solid histogram). The distributions are normalised either the total or the maximum number of stars in each distribution (*left and right panels*, respectively).

regions– with a constant radial gas flow leads to a steepening of the gradient in time.

In the upper panel of Figure 3 we show the $[\text{O}/\text{Fe}]$ vs $[\text{Fe}/\text{H}]$ relations obtained with model REF1 at different Galactocentric distances, spanning the range between 4 and 16 kpc. The theoretical predictions are very similar to the ones reported by Minchev et al. (2013; see their figure 4, bottom left panel) and are mainly driven by the adoption of a SFE that varies with the Galactocentric distance in the model. For reference, we also plot data for solar neighbourhood thin-disc stars by Bensby et al. (2005). In the lower panel of Figure 3 we show the effects of assuming a constant SFE (model REF2) on the $[\text{O}/\text{Fe}]$ vs $[\text{Fe}/\text{H}]$ diagram. It is immediately seen that the observed spread in the data can not be longer reproduced by the chemical evolution model. We conclude that the hypothesis of stellar migration as a solution for the observed spread requires necessarily a variable SFE. This is even more evident from Figure 4, where we show the age-metallicity relation predicted by model REF1 for different Galactocentric distances, compared to the data for thin-disc stars in the solar vicinity from Bensby et al. (2014). Other authors already claimed (e.g. François & Matteucci 1993; Schönrich & Binney 2009a) that the observed spread in the data can be explained with the migration of stars both from the inner and the outer regions, and we confirm their findings. Also, we remark that, while the migration produces a spread of up to 1 dex in $[\text{Fe}/\text{H}]$ at a given age, a much lower spread is expected in the $[\text{O}/\text{Fe}]$ ratios at a given metallicity (cfr. Figures. 3 and 4), in agreement with what is suggested from the observations (see Edvardsson et al. 1993, who first discussed the conundrum of a large spread in the age-metallicity relation apparently contrasting with the tightness of the $[\text{element}/\text{Fe}]$ versus $[\text{Fe}/\text{H}]$ relations for

solar neighbourhood stars).

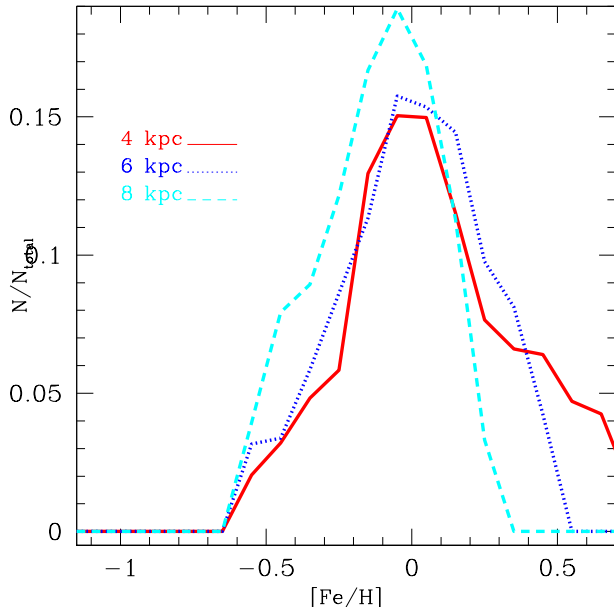


FIG. 7.— The G-dwarf metallicity distributions predicted by model REF1 at 4, 6, and 8 kpc, assuming radial gas flows and no stellar migration.

In Figure 5 we compare the metallicity distribution function of long-lived, thin-disc stars predicted by model REF1 (dashed line) to the observed ones from Adibekyan et al. (2013; solid histogram) and Fuhrmann (2011; dashed histogram). The sample of Adibekyan et al. (2013), comprising stars with Galactocentric distances between 7.9 and 8.1 kpc and with heights above the Galactic plane $|Z|$ smaller than 0.1 kpc, is not a pure thin-disc sample. However, thin-disc stars can be separated from the rest of the sample based on a chemical criterion (the $[\alpha/\text{Fe}]$ vs $[\text{Fe}/\text{H}]$ plot; see Adibekyan et al. 2013). The distributions of Adibekyan et al. (2013) and Fuhrmann (2011), while agreeing on the position of the peak, significantly differ in shape. This could be due to sample selection effects: while Fuhrmann’s survey is limited to objects with *Hipparcos* data within 25 pc from the Sun, Adibekyan et al. (2013) rely on high-resolution analysis of a kinematically unbiased sample of more than 1000 FGK stars located up to 600 pc –but mostly within 50 pc– from the Sun. Interestingly, the APOGEE distribution, extending to significantly larger distances and sampling nearly 10 times more stars, compares well to that from Adibekyan et al. (2013; see Anders et al. 2014). Therefore, in the following we will use the Adibekyan et al. (2013) distribution for comparison with the model predictions. We also recall that our Galactic chemical evolution model is a ‘sequential’ one, and that we consider as thin-disc stars only those with $[\text{Fe}/\text{H}] \geq -0.6$ dex. We see that the metallicity distribution function of Adibekyan et al. (2013) is fairly well reproduced by our model with radial gas inflow and no stellar migration. However, we note that the model underestimates the high-metallicity tail of observed distribution. In Figure 5, the theoretical and observed metallicity distribution functions are normalised to the corresponding

maximum number of stars for each distribution. If we normalise the distributions to the total number of stars (see Figure 6, *left panel*), a good agreement is still found between model predictions and observations.

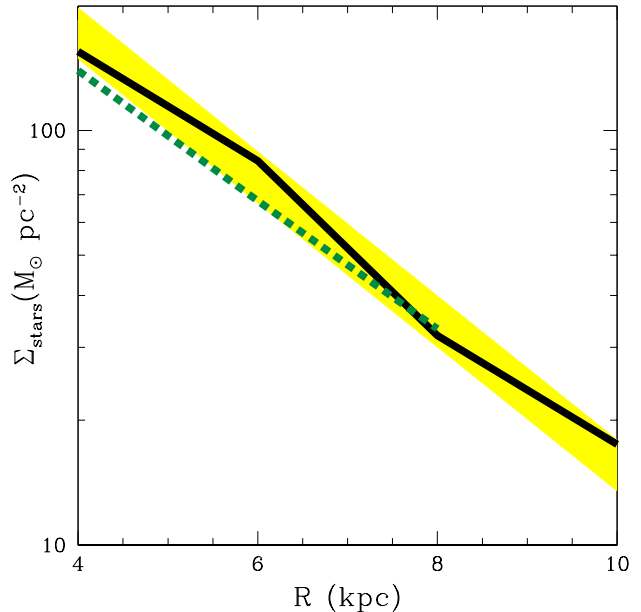


FIG. 8.— The stellar surface density profile predicted by the chemical evolution model REF1 is shown as a black solid line. The green dashed line represents a model in which stellar migration is included according to the results of chemo-dynamical simulations by Minchev et al. (2013; model labeled ‘Minchev case’ in Table 1): 10% (20%) of the stars born at 4 kpc (6 kpc) move toward 8 kpc, whereas 60% of the stars born at 8 kpc leave the solar neighbourhood. The yellow stripe indicates the area spanned by the observational data (see text).

In Figure 7 we show the G-dwarf metallicity distributions obtained by model REF1 at 4, 6, 8 kpc distance from the Galactic centre. As expected, the relative number of high-metallicity stars increases going towards the Galactic center, due to the faster evolution and more efficient star formation in the inner regions. These predictions can be compared to data from large spectroscopic surveys, such as APOGEE and Gaia-ESO, that are mapping increasingly larger volumes of the Milky Way disc (e.g., $5 < R < 11$ kpc, $0 < |Z| < 2$ kpc, Nidever et al. 2014 –APOGEE; $4 < R < 12$ kpc, $0 < |Z| < 3.5$ kpc, Mikolaitis et al. 2014 –Gaia-ESO Survey).

Finally, in Figure 8, the current stellar surface density profile predicted by model REF1 is reported as a black solid line. To compare our model predictions with the relevant data (yellow stripe in the plot), we consider a local stellar density of $35 \pm 5 M_{\odot} \text{pc}^{-2}$ (Gilmore, Wyse & Kuijken 1989) and assume that the stellar profile decreases exponentially outward, with a characteristic length scale of 2.5 kpc (Sackett 1997).

We stress that all the abundance ratios presented in this section are normalized to our theoretical solar abundances, namely the abundances predicted in the ISM at 8 kpc 4.5 Gyr ago. In Section 4 we will use the same normalization.

4. MODEL RESULTS IN THE PRESENCE OF STELLAR MIGRATION

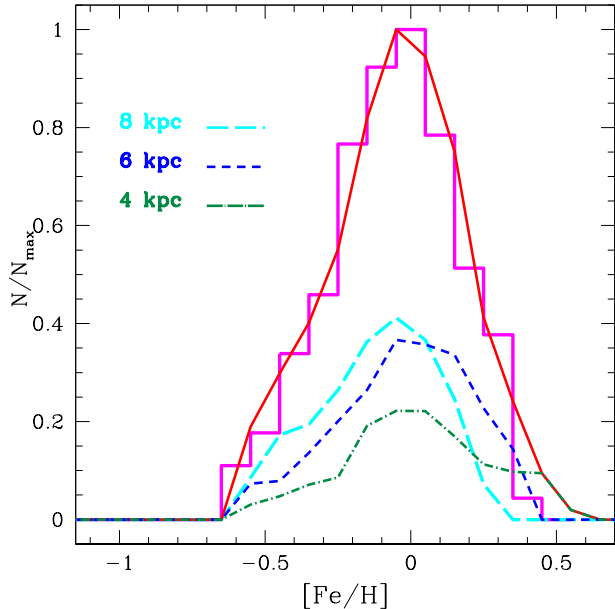


FIG. 9.— Red solid line: theoretical G-dwarf metallicity distribution obtained with the ‘Minchev case’ model, that assumes radial gas flows and stellar migration according to the following recipe: 10% and 20% of the stars born at 4 and 6 kpc, respectively, move toward 8 kpc, whereas 60% of the stars born in situ leave the solar neighbourhood; the stars are assigned a velocity of 1 km s^{-1} . The contributions of the stars born at different Galactocentric radii are also shown (legend on top left corner). The data (magenta histogram) are from Adibekyan et al. (2013).

We now move to illustrate the results of the models that include radial stellar migration. First, we set some simple rules to make stars travel across the disc, somehow mimicking the results of more complex, self-consistent chemo-dynamical models (Minchev et al. 2013): we assume that 10% of the stars born at 4 kpc and 20% of those born at 6 kpc migrate toward 8 kpc, while 60% of those born in the solar neighbourhood migrate (both outwards and inwards); the migrating stars have a velocity of 1 km s^{-1} . We refer to this model as ‘Minchev case’ model (see Table 1). The metallicity distribution function of long-lived solar neighbourhood stars obtained with this model is reported in Figure 9 (red solid line). It is clear that we are now able to explain not only the peak and left wing of the observed distribution (magenta histogram; Adibekyan et al. 2013), but also its high-metallicity tail. We also show in Figure 9 the separate contributions of stars born at 4 and 6 kpc that end up in the solar neighbourhood (green dot-dashed and blue dashed lines, respectively), as well as that of stars born in situ (light blue dashed line). By comparing this figure with figure 3 (middle panel) of Minchev et al. (2013), we note that our model is entirely consistent with their results in terms of the G-dwarf metallicity distribution. The stellar surface density profile that is obtained with the above prescriptions for stellar migration is presented in Figure 8 (green dashed line). The observed profile (yellow stripe) is reproduced and the model leads to a stellar surface density of $33 M_{\odot} \text{ pc}^{-2}$ in the solar neighbourhood, in agreement with the observed value.

In Figure 10, we explore the effects of different assumptions about the velocities of the migrating stars on the

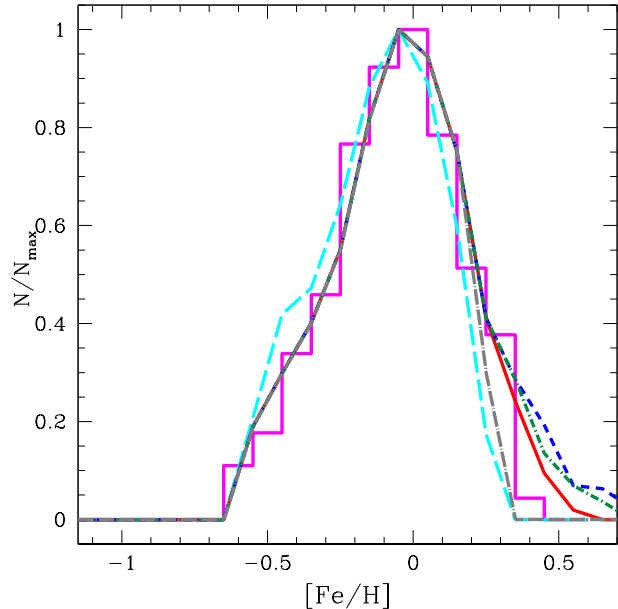


FIG. 10.— Effects of different prescriptions about the velocity of the migrating stars on the metallicity distribution of solar neighbourhood long-lived stars predicted with the ‘Minchev case’ model. The short-dashed blue line represents the model results when the finite velocity of the stars is not taken into account. The solid red and short-dashed-dotted green lines refer to adopted velocities of 1 and 2 km s^{-1} , respectively, while the long-dashed-dotted grey line stands for a case in which the stellar velocity is set to 0.5 km s^{-1} . With the long-dashed cyan line we also show our reference model (REF1) without stellar migration. The data (magenta histogram) are for thin-disc stars from Adibekyan et al. (2013).

predicted G-dwarf metallicity distribution (the stars migrate according to the scheme discussed in the previous paragraph). We either do not take the stellar velocity into account, or analyse cases in which stellar velocities of 0.5 , 1 and 2 km s^{-1} are considered. The observed G-dwarf metallicity distribution is best reproduced with a velocity of 1 km s^{-1} . Adopting a smaller velocity (e.g. 0.5 km s^{-1}) has the consequence that many more stars among the ones born more recently and at larger distances from the solar neighbourhood have not sufficient time to reach the solar vicinity, compared to models which assume larger stellar velocities. As a result, the right tail of the Adibekyan et al. (2013) distribution is no more reproduced, and the model tends to the case without stellar migration.

Kobayashi & Nakasato (2011) presented chemo-dynamical simulations of a Milky-Way-type galaxy using a self-consistent hydrodynamical code that includes supernova feedback and chemical enrichment, and predicts the spatial distribution of elements from oxygen to zinc. With their model they predict that only 30% of the stars which reside in the solar neighbourhood has originated from different regions of the Galactic disc (C. Kobayashi, private communication). In Minchev et al. (2013) study, approximately 60% of the stars currently found in the solar neighbourhood would have formed at 4 and 6 kpc. Therefore, so far, it is not possible to reach firm conclusions about the effective amount of stellar migration in the Galactic disc. It is interesting to note, as already pointed out by previous authors, that stellar migration brings to the solar neighbourhood a few

old, metal-rich stars, thus fulfilling the requirements implied by observations of Grenon (1972, 1989). However, it is also important to stress that it does not lead to substantial changes in the theoretical metallicity distribution function of long-living stars, making a quantification of the extent of migration based on this observable a hard task.

Another important issue is that the migrated stars could end up to populate the thick disc in the solar neighbourhood, as indicated by Minchev et al. (2013): in this case, the G-dwarf metallicity distribution would suffer an even smaller effect by migrating stars.

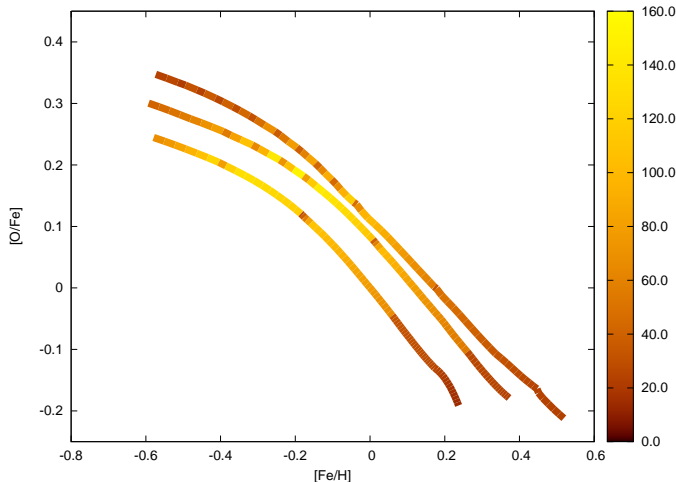


FIG. 11.— $[O/Fe]$ vs $[Fe/H]$ in the solar neighbourhood for the ‘Minchev case’ model, where a velocity of 1 km s^{-1} is considered for the migrating stars. The lines are color-coded according to the number of stars (in unit of 10^6). The upper curve refers to stars born at 4 kpc, the middle one to stars born at 6 kpc, the lower curve represents stars born in situ.

We compute the numbers of stars in the solar neighbourhood that are expected to have a given $[O/Fe]$ at a given $[Fe/H]$, as well as the numbers of stars with a certain $[Fe/H]$ at a given age, for the ‘Minchev case’ model taking into account a stellar velocity of 1 km s^{-1} (see Figures 11 and 12, respectively). In Figure 12 it is clearly shown the effect of setting the velocity of the stars to a fixed value. We are considering velocities fixed at $1 \text{ km s}^{-1} \approx 1 \text{ kpc Gyr}^{-1}$ and, thus, the curve relative to the stars coming from 4 kpc ends at 10 Gyr: all stars born at 4 kpc at times larger than 10 Gyr from the beginning of the simulation do not have enough time to reach the solar neighbourhood. The same explanation is valid for the 6 kpc line result, i.e. for times larger than 12 Gyr no stars formed at 6 kpc can reach the solar neighbourhood.

In Figure 13 we show the metallicity distributions of long-lived stars in the solar vicinity predicted by our models with (dashed lines; ‘Minchev case’ model, velocity of the migrating stars set to 1 km s^{-1}) and without stellar migration (solid lines; model REF1). The total distributions (cyan lines) are split in different age bins: we consider young stars (ages $< 1 \text{ Gyr}$; blue lines), intermediate-age stars ($1 \text{ Gyr} < \text{ages} < 5 \text{ Gyr}$; black lines) and old stars (ages $> 5 \text{ Gyr}$; red lines). Each distribution is normalised to the total number (young+intermediate+old) of stars. The finite velocity of the stars is taken into account in order to establish how

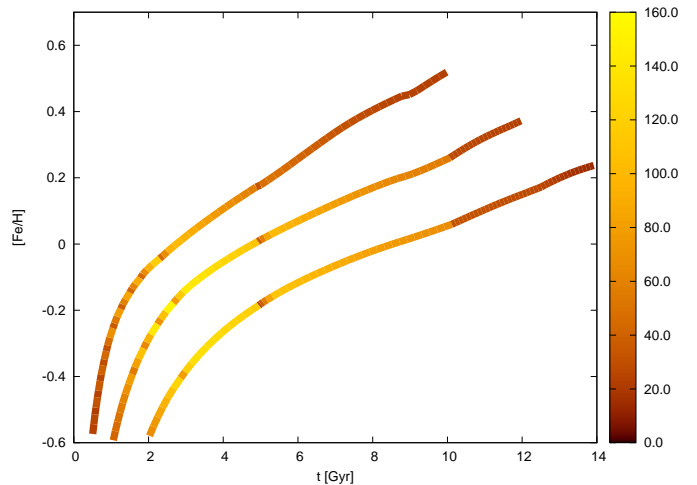


FIG. 12.— $[Fe/H]$ vs time in the solar neighbourhood for the ‘Minchev case’ model, where a velocity of 1 km s^{-1} is considered for the migrating stars. The lines are color-coded according to the number of stars (in unit of 10^6). The upper curve refers to stars born at 4 kpc, the middle one to stars born at 6 kpc, the lower curve represents stars born in situ.

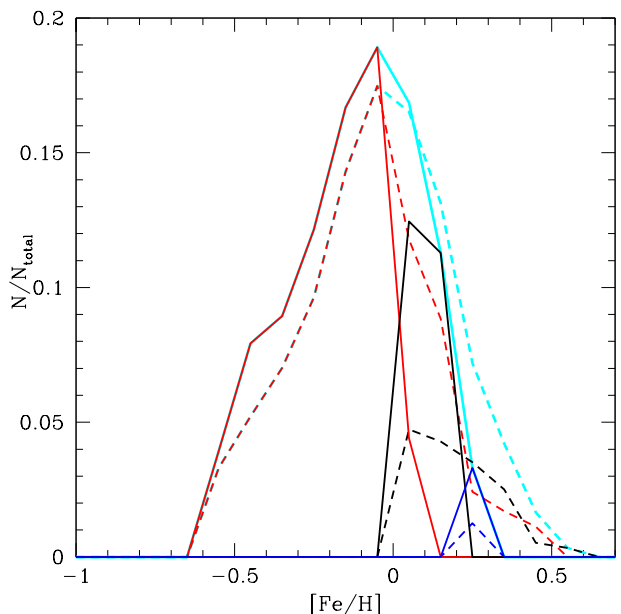


FIG. 13.— G-dwarf metallicity distributions at 8 kpc obtained by our models for young stars (ages $< 1 \text{ Gyr}$; blue lines), intermediate-age stars ($1 \text{ Gyr} < \text{ages} < 5 \text{ Gyr}$; black lines) and old stars (ages $> 5 \text{ Gyr}$; red lines). The cyan lines show the sum of all age distributions. The solid lines refer to model REF1, without stellar migration but including radial gas flows. The dashed lines refer to the ‘Minchev case’ model with velocity of the migrating stars fixed at 1 km s^{-1} . Each distribution is normalised to the total number (young+intermediate+old) of stars.

many inner-disc stars end up in the solar neighbourhood.

In our reference model without stellar migration (model REF1, with variable SFE and radial gas inflow included with a velocity of 1 km s^{-1}), 3.30% of the stars present ages less than 1 Gyr, 23.74% have ages between 1 and 5 Gyr, whereas the oldest stars with ages larger than 5 Gyr are 72.96% of the total. Concerning the model with stellar migration (‘Minchev case’ model), 1.25% of the stars have ages less than 1 Gyr, 15.93% have ages be-

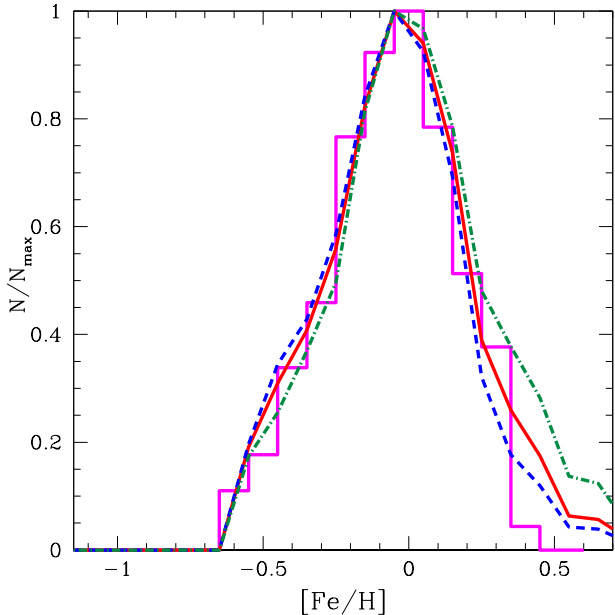


FIG. 14.— G-dwarf metallicity distributions predicted by our ‘extreme’ models where stars born in situ at 8 kpc are not allowed to migrate. The dashed blue line refers to the predictions of case 1) migration (10% and 20% of the stars born at 4 and 6 kpc, respectively, end up at 8 kpc). Case 2) migration (20% and 40% of the stars born at 4 and 6 kpc, respectively, end up at 8 kpc) is represented by the solid red line and case 3) migration (all stars born at 4 and 6 kpc end up at 8 kpc) is represented by the green dashed-dotted line. The observed distribution of thin-disc stars (magenta histogram) is taken from Adibekyan et al. (2013).

tween 1 and 5 Gyr, and the oldest stars with ages larger than 5 Gyr are 82.82%. Different prescriptions for the stellar velocities would increase (smaller velocities) or decrease (larger velocities) the contribution of the old stars to the G-dwarf metallicity distribution function. The main effect of the stellar migration, in the way in which it is implemented here, is to increase the percentage of old stars in the solar neighbourhood compared to the model without stellar migration.

Finally, we test the effects on the metallicity distribution of long-lived stars in the solar neighbourhood of ‘extreme’ stellar migrations, where we do not allow stars born in situ at 8 kpc to migrate toward other regions. We distinguish 3 cases:

- case 1): 10% of the stars born at 4 kpc and 20 % of those born at 6 kpc migrate towards 8 kpc;
- case 2): 20% of the stars born at 4 kpc and 40 % of those born at 6 kpc migrate towards 8 kpc;
- case 3): all the stars born at 4 and 6 kpc migrate towards 8 kpc.

We show (Figure 14) that the main effect of stellar migration in all these extreme cases (even in the really extreme and unphysical case 3) is to populate the high-metallicity tail of the predicted distribution. Overall, the

predicted stellar metallicity distribution is not substantially affected. In particular, the position of the peak is left unchanged: it mostly depends on the assumed timescale of thin-disc formation. We conclude that the G-dwarf metallicity distribution cannot be used to extract information on the extent and significance of stellar migration. However, this process is clearly needed in order to improve the agreement between model predictions and observations on the high-metallicity tail.

5. CONCLUSIONS

In this paper we have studied the effects of the stellar migration by means of a detailed chemical evolution model where radial gas flows in the galactic disc are also considered. The stellar migration is implemented in the code in a phenomenological way, just mimicking the results of published dynamical models, with no intention of studying the physics of this phenomenon. Our main conclusions can be summarized as follows:

- Our reference chemical evolution model for the thin disc of the Milky Way, assuming a variable star formation efficiency, a constant radial gas inflow (fixed at -1 km s^{-1}) and no stellar migration, is able to well fit the majority of the observables: the abundance gradient along the Galactic disc, the stellar mass surface density profile; also the observed G-dwarf metallicity distribution of thin-disc stars (Adibekyan et al. 2013) is generally in agreement with our model, the only problem residing in the high-metallicity tail of the distribution, which our model is underestimating.
- By including stellar migration according to simple prescriptions that mimic the results of chemodynamical models by Minchev et. al. (2013), and taking into account velocities of 1 km s^{-1} for the migrating stars, we are able to reproduce very well the high-metallicity tail of the G-dwarf metallicity distribution observed for thin-disc stars.
- By exploring the velocity space, we conclude that the stellar migration velocities must have values larger than 0.5 km s^{-1} and smaller than 2 km s^{-1} to properly reproduce the high-metallicity tail in the G-dwarf metallicity distribution of thin-disc stars.
- As found by previous authors (François & Matteucci 1993; Schönrich & Binney 2009a; Minchev et al. 2013) the observed spread, if real, in $[\text{O}/\text{Fe}]$ vs $[\text{Fe}/\text{H}]$, and age vs $[\text{Fe}/\text{H}]$ relations, can be partially explained by taking stellar migration into account. We proved that the hypothesis of stellar migration as a solution for the observed spread requires necessarily a variable SFE.

ACKNOWLEDGMENTS

We thank the anonymous referee for his/her suggestions that have improved the paper. We acknowledge financial support from PRIN MIUR 2010-2011, project ‘The Chemical and Dynamical Evolution of the Milky Way and Local Group Galaxies’, prot. 2010LY5N2T.

REFERENCES

- Bensby, T., Feltzing, S., Lundstrom, I. & Ilyin, I. 2005, *A&A*, 433, 185
- Bensby, T., Fetzling, S. & Oey, M. S. 2014, *A&A*, 562, A71
- Bilitewski, T. & Schönrich, R. 2012, *MNRAS*, 426, 2266
- Cavichia, O., Mollá, M., Costa, R. D. D. & Maciel, W. J. 2014, *MNRAS*, 437, 3688
- Chiappini, C., Matteucci, F. & Gratton, R. 1997, *ApJ*, 477, 765
- Chiappini, C., Matteucci, F. & Romano, D. 2001, *ApJ*, 554, 1044
- Colavitti, E., Matteucci, F. & Murante, G. 2008, *A&A*, 483, 401
- Dehnen, W. 2000, *AJ*, 119, 800
- Edvardsson, B., Andersen, J., Gustafsson, B., et al. 1993, *A&A*, 275, 101
- François, P. & Matteucci, F. 1993, *A&A*, 280, 136
- François, P., Matteucci, F., Cayrel, R., et al. 2004, *A&A*, 421, 613
- Fuhrmann, K. 2011, *MNRAS*, 414, 2893
- Gilmore, G., Wyse, R. F. G. & Kuijken, K. 1989, *ARA&A*, 27, 555
- Goetz, M. & Koepfen, J. 1992, *A&A*, 262, 455
- Greggio, L. & Renzini, A. 1983, *A&A*, 118, 217
- Grenon, M. 1972, in *IAU Colloq. 17: Age des Etoiles*, eds. G. Cayrel de Strobel, & A. M. Delplace (Meudon: Observatoire de Paris), 55
- Grenon, M. 1989, *Ap&SS*, 156, 29
- Halle, A., Di Matteo, P., Haywood, M. & Combes, F. 2015, arXiv:1501.00664, submitted to *A&A*
- Iwamoto, K., Brachwitz, F., Nomoto, K., et al. 1999, *ApJ Suppl. Ser.*, 125, 439
- Kennicutt, R. C., Jr. 1998, *ApJ*, 498, 541
- Kobayashi, C. & Nakasato, N. 2011, *ApJ*, 719, 16
- Kordopatis, G., Gilmore, G., Steinmetz, M., et al. 2013, *AJ*, 146, 134
- Kubryk, M., Prantzos, N. & Athanassoula, E. 2013, *MNRAS*, 436, 1479
- Kubryk, M., Prantzos, N. & Athanassoula, E. 2014, arXiv:1412.0585, submitted to *A&A*
- Lacey, C. G. & Fall, M. 1985, *ApJ*, 290, 154
- Larson, R. B. 1976, *MNRAS*, 176, 31
- Luck, R. E. & Lambert, D. L. 2011, *AJ*, 142, 136
- Maeder, A. & Meynet, G. 1989, *A&A*, 210, 155
- Matteucci, F. 2001, *The Chemical Evolution of the Galaxy* (Astrophysics and Space Science Library, Vol. 253; Dordrecht: Kluwer)
- Matteucci, F. & François, P. 1989, *MNRAS*, 239, 885
- Matteucci, F. & Greggio, L. 1986, *A&A*, 154, 279
- Mikolaitis, Š., Hill, V., Recio-Blanco, A., et al. 2014, *A&A*, 572, A33
- Minchev, I., Chiappini, C. & Martig, M. 2013, *A&A*, 558, A9
- Minchev, I., Chiappini, C. & Martig, M. 2014, *A&A*, 572, A92
- Minchev, I. & Famaey, B. 2010, *ApJ*, 722, 112
- Minchev, I., Famaey, B., Combes, F., et al. 2011, *A&A*, 527, 147
- Mott, A., Spitoni, E. & Matteucci, F. 2013, *MNRAS*, 435, 2918
- Nidever, D. L., Bovy, J., Bird, J. C., et al. 2014, *ApJ*, 796, 38
- Portinari, L. & Chiosi, C. 2000, *A&A*, 355, 929
- Romano, D., Chiappini, C., Matteucci, F. & Tosi, M. 2005, *A&A*, 430, 491
- Röskar, R., Debattista, V. P., Quinn, T. R., Stinson, G. S. & Wadsley, J. 2008, *ApJ*, 684, L79
- Röskar, R., Debattista, V. P., Quinn, T. R. & Wadsley, J. 2012, *MNRAS*, 426, 2089
- Sackett, P. D. 1997, *ApJ*, 483, 103
- Sánchez-Blázquez, P., Rosales-Ortega, F., Méndez-Abreu, J., et al. 2014, *A&A*, 570, A6
- Scalo, J. M. 1986, *FCPh*, 11, 1
- Schönrich, R. & Binney, J. 2009a, *MNRAS*, 396, 203
- Schönrich, R. & Binney, J. 2009b, *MNRAS*, 399, 1145
- Sellwood, J. A. & Binney, J. J. 2002, *MNRAS*, 336, 785
- Smet, C., Posacki, S. & Ciotti, L. 2014, arXiv:1412.4794, accepted for publication in *MNRAS*
- Spitoni, E. & Matteucci, F. 2011, *A&A*, 531, A72
- Spitoni, E., Matteucci, F. & Marcon-Uchida, M. M. 2013, *A&A*, 551, A123
- van den Hoek, L. B. & Groenewegen, M. A. T. 1997, *A&AS*, 123, 305
- Vera-Ciro, C., D’Onghia, E., Navarro, J. & Abadi, M. 2014, *ApJ*, 794, 173
- Woosley, S. E. & Weaver, T. A. 1995, *ApJ*, 101, 181
- Wyse, R. F. G. & Silk, J. 1989, *ApJ*, 339, 700